Published in final edited form as:
J Control Release. 2010 March 19; 142(3): 326–331. doi:10.1016/j.jconrel.2009.10.037.

LIPOSOMAL MODULAR COMPLEXES FOR SIMULTANEOUS TARGETED DELIVERY OF BIOACTIVE GASES AND THERAPEUTICS

Melvin E. Klegerman[1,*,†], **Michael Wassler**[1], **Shao-Ling Huang**[1], **Yuejiao Zou**[1], **Hyunggun Kim**[1], **Harnath S. Shelat**[1], **Christy K. Holland**[2], **Yong-Jian Geng**[1], and **David D. McPherson**[1]

[1]Division of Cardiology, Department of Internal Medicine, University of Texas Health Science Center, 6431 Fannin Street, MSB 1.246, Houston, Texas 77030, U.S.A.

[2]Department of Biomedical Engineering, University of Cincinnati, 231 Albert Sabin Way, 10 Medical Sciences Building, Room 6152, Cincinnati, Ohio 45267, U.S.A.

Abstract

Intrinsically echogenic liposomes (ELIP) can be adapted to encapsulate nitric oxide to facilitate ultrasound-enhanced delivery of therapeutic agents to atherosclerotic plaques. However, the NO loading of targeted ELIP caused a 93% decrease of antibody (Ab) immunoreactivity. The following hypothesis was tested: biotin/avidin-mediated coupling of NO-ELIP and Ab-conjugated ELIP will enable co-delivery of bioactive gases and ELIP that can encapsulate other agents without loss of targeting efficiency. Complex formation was initiated by addition of excess streptavidin to equal proportions of biotinylated Ab-ELIP and NO-ELIP. Fluorescence deconvolution microscopy, Coulter Multisizer 3 analysis and flow cytometry demonstrated that the ELIP coupling procedure formed mixed aggregates of ≥10 liposomes within 1 minute. Intravascular ultrasound imaging and ELISA showed that echogenicity and targeting efficiency were completely and 69–99% retained, respectively. When complexed to NO-ELIP, ELIP bifunctionally targeted to both CD34 and ICAM-1 (BF-ELIP) increased human mononuclear cell migration through human coronary artery endothelial cell monolayers in transwell plates 4-fold relative to a nonspecific IgG-ELIP control and 2-fold relative to BF-ELIP alone. It was concluded that this novel multi-functional conjugation methodology provides a platform technology for site-specific co-delivery of bioactive gases and other agents.

Keywords

Liposomes; Bioactive Gases; Atherosclerosis; Stem Cells; Ultrasound

1. Introduction

Nitric oxide (NO) is a potent bioactive gas with vasodilatory, anti-inflammatory, anti-thrombotic and antiproliferative properties that has been shown to possess anti-atherogenic

*To whom correspondence should be addressed. Phone: 1-713-500-2343; FAX: 1-713-500-2325; Melvin.E.Klegerman@uth.tmc.edu.
†Dr. Melvin Klegerman has research-related interests in EchoDynamics, Inc.

activity [1,2]. Several vascular diseases have been ameliorated by administration of NO precursors, synthetic NO promoters such as L-arginine, the endothelial NO synthase (eNOS) gene, NO donors and NO gas [3–5]. The latter administrative route has been approved for the treatment of chronic pulmonary hypertension in the U.S.[6], but efficacy is limited by rapid dissipation and clearance of the gas, systemic side-effects and endogenous NO scavengers such as hemoglobin [5].

A number of formulations for molecular imaging and drug and gene delivery have been developed using the intrinsically echogenic liposome (ELIP) technology [7–12]. The encapsulation of air into these liposomal formulations results in a contrast agent that is suitable for ultrasound image enhancement and controlled release of therapeutic agents, while being stable in the circulation for a prolonged period [8]. Liposomal encapsulation of NO has been achieved by modifying the ELIP preparation procedure, retaining the formulation's echogenic properties, while obviating the drawbacks of NO gas delivery [13]. The resultant NO-ELIP formulation encapsulated 10μl NO gas/mg lipid, 50% of which was released during the first 10 minutes, with the remainder being released more slowly over the ensuing 8 hours. The release rate could be modulated by diluting the NO in the formulation with argon gas. The encapsulated NO was effectively sequestered from hemoglobin scavenging and local administration of NO-ELIP significantly inhibited development of neointimal hyperplasia in a rabbit atherogenesis model [13].

A major advantage of the ELIP formulation is that these liposomes can be readily targeted to pathologic structures by conjugation of antibodies and other ligands to the phosphatidyl ethanolamine head groups [9,14–16]. Preliminary studies have demonstrated, however, that conjugation of antibodies directly to NO-loaded ELIP resulted in >90 percent loss of antibody immunoreactivity, mainly due to protein denaturation induced by gas pressurization and freeze-thawing procedures (previously unpublished results). This study addresses a novel approach to simultaneous delivery of bioactive gases and, by extension, therapeutic agents, using a targeted ELIP platform with minimal loss of targeting efficiency.

2. Materials and Methods

2.1. Preparation of standard ELIP

A 27:42:8:8:15 molar ratio of the lipid components L-α-phosphatidylcholine (chicken egg; EPC), 1,2-dipalmitoyl-*sn*-glycero-3-phosphocholine (DPPC), 1,2-dipalmitoyl-*sn*-glycero-3-[phosphor-rac-1-glycerol] (DPPG), 1,2-dipalmitoyl-*sn*-glycero-3-phosphoethanolamine (DPPE), and cholesterol (CH) were mixed in a round-bottom flask as chloroform solutions. For preparation of fluorescent ELIP, 0.2 mole% lissamine rhodamine B-DPPE or carboxyfluorescein-dioleoyl PE (Avanti Polar Lipids) was included in the formulation, which was subsequently protected from exposure to light. The chloroform was then removed by evaporation under argon, while the flask was rotated in a 50°C water bath. The resulting lipid film was placed under vacuum for 4 hours at ≤100 mTorr pressure for complete removal of the solvent, followed by rehydration of the dry lipid film with 0.32 M mannitol to a concentration of 10 mg lipid/ml. The hydrated lipid was incubated at 55°C for 30 minutes to ensure that all lipids were in the liquid phase during hydration. The mixture was then sonicated in a water bath for 5 minutes. Aliquots of the suspension were frozen at −80°C and lyophilized for 24–48 hours. Each lyophilized dry cake was resuspended with the original volume of nanopure water immediately before use.

2.2. Preparation of NO-ELIP

Liposomes of the above composition were prepared according to a previously developed pressurization-freeze method [13]. Briefly, after drying and hydrating the lipid film, 300-μl

aliquots of the suspension were transferred to 2-ml borosilicate glass vials (12×32 mm), which were then sealed with Teflon-coated silicon rubber septal screw caps. Nitric oxide (5.4 ml STP), washed and purified by passage through a saturated sodium hydroxide solution in order to remove nitrogen dioxide produced by contaminating oxygen, or a mixture of NO and argon was introduced into each vial through the septum and pressurized to 9 atm using a syringe fitted with a 27G×1/2" needle. The pressurized gas/liposome dispersion was incubated for 30 minutes at room temperature, followed by freezing on dry ice for ≥ 30 minutes. Vials were stored at −80° C. Prior to use, the pressure was released by loosening the caps immediately after removal from storage, followed by thawing of the NO-ELIP suspension at room temperature.

2.3. Preparation of control, fibrinogen and bifunctional (stem cell and ICAM-1) targeted ELIP

For conjugation, anionic ELIP were prepared as described above, substituting 1,2-dipalmitoyl-sn-glycero-3-phosphoethanolamine-N-[4-(*p*-maleimidophenyl) butyrate] (MPB-PE) for PE. For preparation of bifunctional targeted ELIP (BF-ELIP), monoclonal anti-human/mouse ICAM-1 (0.2 mg) + 0.2 mg rabbit anti-human/mouse CD34 (both from Santa Cruz Biotechnology, Inc.) + 1.6 mg nonspecific mouse IgG were reacted with 3-(2-pyridyldithiolpropionic acid)-N-hydroxysuccinimide ester (SPDP) at a SPDP-protein molar ratio of 15:1 for 30 min at room temperature (RT). For a control preparation, 2 mg of nonspecific IgG was used without specific antibody (Ab). For fibrinogen targeting, 2 mg of rabbit anti-human fibrin(ogen) Ab (American Diagnostica, Inc.) was utilized. Protein was separated from unreacted SPDP by gel chromatography on a 50 ml Sephadex G-50 column equilibrated with 0.05M citrate-phosphate buffer, pH 5.5. Protein fractions were identified (optical absorbance at 280 nm, A_{280}), pooled and concentrated to ≤ 2ml using Centricon YM-10 centrifugal filter units. The PDP-protein was reduced in 25mM dithiothreitol (DTT) for 30 min at RT. The thiolated protein was isolated (G-50 column), equilibrated and eluted with pH 6.7 citrate-phosphate buffer. Protein-containing fractions were pooled and concentrated. The thiolated protein was reacted with 30 mg of reconstituted MPB-ELIP (10mg lipid/ml 0.1M phosphate buffer, pH 6.62) under argon overnight at RT. Conjugated ELIP were separated from free protein and low molecular weight products by gel filtration on a 20-ml Sepharose CL-4B column that had been pre-saturated with unconjugated ELIP according to the method of Lasch *et al.* [17,18] and eluted with 0.02M phosphate-buffered saline (PBS), pH 7.4. Liposome-containing fractions were identified by optical absorbance at 440 nm prior to elution of free IgG, established during calibration of the column. The pooled liposome fraction was lyophilized in the presence of 0.1M D-mannitol. Conjugation efficiency (CE; in μg Ab/mg lipid) of IgG- or Ab-ELIP was determined by quantitative immunoblot assay [19] relative to a composite curve of IgG-ELIP secondary standards. Ab-ELIP size distribution and number were determined with a Coulter Multisizer 3, fitted with a 20 μm aperture tube, which permits sizing down to 400 nm equivalent spherical diameter. Based on the number of liposomes, CE is also expressed as number of Ab molecules per liposome.

2.4. Liposome biotinylation and complex formation

ELIP were prepared with 8 mole% biotinyl-DPPE (instead of DPPE) for NO loading and with 2 mole% biotinyl-PE (in addition to the 8 mole% MPB-PE, while decreasing the DPPC content by 2 mole%) for IgG or Ab conjugation. Complex formation was initiated by addition of excess streptavidin (a 20 μg/ml solution equal in volume to the IgG-ELIP component) to equal proportions (by weight) of the two preparations.

2.5. Enzyme-linked immunosorbent assay (ELISA) characterization of fibrinogen-targeted and bifunctional ELIP

The direct ELISA protocol for evaluation of fibrinogen-targeted ELIP was described previously [17]. A sandwich ELISA protocol was used to determine the antiICAM-1

immunoreactivity of BF-ELIP. Nunc MaxiSorp microtiter plates were coated with 5 μg/ml of a polyclonal anti-human ICAM-1 capture Ab (R&D Systems) in 0.05M sodium bicarbonate, pH 9.6, overnight at 4°C. All incubation volumes were 50 μl/well. One-third of wells were left uncoated for determination of nonspecific binding. After aspirating well contents, all wells were blocked with conjugate buffer (1% bovine serum albumin in 0.05M Tris buffer, pH 8.0, with 0.02% sodium azide) for 1 hour. All incubations were at 37°C. Each incubation was followed by aspiration of well contents and washes (3X) with PBS-T (0.02M phosphate-buffered saline, pH 7.4, with 0.05% Tween 20). All wells were then incubated with 200 ng/ml of recombinant soluble human ICAM-1 (Bender MedSystems) in 0.1% BSA/PBS-T diluent for 2 hours. For assay of intact Ab-ELIP, wells were washed with PBS after this incubation and the first wash after the Ab-ELIP incubation was also with PBS. Various dilutions of antiICAM-1 Ab and Ab-ELIP (both in PBS) were incubated for 1 hour, followed by a 1-hour incubation with 1:1,000 goat anti-mouse IgG-alkaline phosphatase (Bio-Rad Laboratories) in conjugate buffer. The substrate incubation consisted of 50 μl of substrate buffer (0.05M glycine buffer, pH 10.5, with 1.5mM magnesium chloride) + 50 μl *p*-nitrophenyl phosphate (Sigma Chem. Co.; 4 mg/ml) in substrate buffer per well for 15 minutes. The reaction was stopped with 50 μl 1M sodium hydroxide per well.

The optical absorbance of each well at 405 nm (A_{405}) was measured with a Tecan Safire^2 microplate reader. Net A_{405} was determined by subtracting the absorbance of background wells from that of capture Ab-coated wells. The dissociation constant (K_D) of Ab-ELIP binding to rshICAM-1 was derived as b of $y = ax/(b + x)$ from a hyperbolic fit of the ELISA data (y = Net A_{405}, ×= [Ab]) performed with SigmaPlot software. Antibody concentration ([Ab]) for Ab-ELIP was calculated from the CE. K_D values were corrected for perturbation of equilibrium conditions during the anti-mouse IgG-AP incubation according to Underwood [17,20]. Loss of immunoreactivity in ELIP complexes was determined by measuring [Ab] relative to the antiICAM-1 standard in the ELISA and setting an Ab-ELIP control (without NO-ELIP or streptavidin) equal to 100 percent immunoreactivity.

2.6. Echogenicity Analysis

The liposomes were imaged with a 15 MHz intravascular ultrasound (IVUS) catheter in a glass vial, utilizing a modified CVIS IVUS system (Boston Scientific Inc.). Relative echogenicity (apparent brightness) of the liposome formulations was objectively assessed using computer-assisted videodensitometry. This process involved image acquisition, pre-processing, and gray scale quantification. All image processing and analyses were performed with Image Pro-Plus Software (Ver. 4.1, Media Cybernetics, Silver Spring, MD). Images were digitized to 640 × 480-pixel spatial resolution (approximately 0.045 mm/pixel) and 8-bit (256 level) gray scale. For a pixel in an 8-bit bitmap image, an intensity value of 0 corresponds to no ultrasound reflectivity (black), while a value of 255 signifies maximal reflectivity (white). Data are reported as mean gray scale values (MGSV).

2.7. Fluorescence Deconvolution Microscopy

Biotinylated IgG-conjugated and NO-loaded ELIP were labeled with rhodamine B and fluorescein, respectively, as described above. A cover slip precoated with 0.1% poly-L-lysine was covered with a fivefold dilution of the mixed liposomal suspension 10 and 30 minutes after initiation of complex formation. After removal of excess fluid, the cover slip was inverted and mounted on a microscope slide with Elvanol anti fade (DuPont, Wilmington, DE). The slides were scanned with an Applied Precision DeltaVision Fluorescence Deconvolution Microscope (Applied Precision, Issaquah, WA), followed by 3D image reconstruction as previously described [21–23]. Image analysis was with SoftWoRxTM software (Applied Precision, Issaquah, WA), using a point-spread function, algorithm method. All data sets were subjected to five deconvolution iterations and then used for image reconstruction and modeling.

Stacking of individual sections produces a three dimensional image on a two dimensional background, resulting in an image projection.

2.8. Flow Cytometry

ELIP complexes were prepared with biotinylated fluorescein-labeled NO-loaded ELIP (NO-bELIP) and unlabeled IgG-bELIP. Two-color analyses were performed on the individual ELIP component controls and the complexes, 5 and 30 minutes after initiation, stained with anti-mouse IgG-phycoerythrin (Novus Biologicals, Littleton, CO), using a FACS Canto II (BD Biosciences), which has 3-laser, 8 color capacity, and BD FACS Diva 6.1.1 software.

2.9. Transwell System for Measurement of BF-ELIP Facilitation of Stem Cell Passage Through Endothelial Cell Monolayers

Human coronary artery endothelial cells (HCAEC) were grown to confluence in 24-well Transwell insert plates (8μm pores; Corning Life Sci., Lowell, MA) and were then pre-treated overnight with TNF-α (20ng/ml IMDM). IgG- or BF-bELIP (120 μg lipid/well), sterilized by ultraviolet light for 60 minutes [24], with and without complexed NO-bELIP (UV-sterilized for 15 minutes), was incubated with the cells for 5 minutes at 37°C in an atmosphere of 5% CO_2/95% air, followed by a single wash with Dulbecco's PBS (DPBS). DAPI-stained or GFP-transfected human peripheral blood mononuclear cells (HMNC), isolated from buffy coat by Ficoll-Paque (Sigma-Aldrich) density gradient centrifugation (4×10^4 cells/well), were added to the wells and allowed to incubate under the same conditions for 5 minutes, followed by a single wash. IMDM (200 μl) was then added to the inserts and the plates were incubated under the same conditions for 24 hours, after which all cells were removed from the apical membrane surface with a cotton swab. Cells that had migrated to the underside of the membrane were examined and enumerated by fluorescence microscopy with a Nikon Eclipse E800 microscope.

2.10. Statistics

SigmaStat (Ver 3.1, Systat Software Inc.) was utilized for statistical analyses. Data groups were subjected to normal variance analysis and were compared by a one-tailed t-test. Immunoreactivity data of treatment groups were compared by one-way ANOVA and the Holm-Sidak method. Proportions of two-color staining liposome preparations in flow cytometry were compared by chi-squared (χ^2) analysis.

3. Results

When BF-ELIP pressurized with NO, as described in the Methods section, was tested for ICAM-1 targeting efficiency in the ELISA, it was found that 93% of Ab immunoreactivity had been lost (Fig. 1). The loss of Ab reactivity was apparently caused mainly by the gas pressurization process, since 86.4 ± 6.1% reactivity was lost after pressurization with argon. Additional incremental losses of immunoreactivity were produced by air and NO pressurization (significantly greater than immunoreactivity after Ar pressurization; $p = 0.0122$), indicating further destructive effects of oxidation and free radical reactions, respectively. Liposomal conjugation of Ab was somewhat protective, since 97% of unconjugated Ab reactivity was lost after NO pressurization (Fig.1).

The biotin/avidin-mediated ELIP modular complex scheme (Fig. 2) was tested with rhodamine B-labeled IgG-ELIP and fluoresceinated NO-loaded ELIP modules. Deconvolution fluorescence microscopy of slides prepared from ELIP suspensions 10 and 30 minutes after complex initiation showed numerous mixed complexes of ≤ 10 - ~500 liposomes (30-minute panels shown in Fig. 3). No consistent pattern of liposomal organization was seen, but some rhodamine-labeled modules were frequently observed at the edge of the complexes, indicating a likelihood that their molecular targeting characteristics would be preserved. Flow cytometry

of 200,000 particles indicated that extensive complexation occurred prior to 5 minutes after initiation, but continued to increase thereafter. Mixed complexes accounted for 0.70% of total particles 5 minutes after initiation, which increased to 1.19% at 30 minutes (Fig. 4). The difference between these two proportions was significant ($\chi^2 = 258$).

Beckman Coulter Multisizer 3 analysis indicated that complex formation was essentially complete within one minute after initiation (Fig. 5). The median spherical diameter of the IgG-bELIP and the NO-bELIP was 737 ± 83 nm (SD, n = 3) and 566 ± 24 nm, respectively. The proportion of new particles > 2 μm in diameter formed within 30 minutes after complex initiation (2.4%) was comparable to the proportion of mixed complexes determined by flow cytometry and may indicate that about half of the total complexes formed contained a single type of liposome. The mean of total particle number after complex formation ($1.68 \pm 0.14 \times 10^{10}$/ml; n = 21) was 21% lower than that of the control preparation ($2.12 \pm 0.19 \times 10^{10}$/ml; n = 9, $p < 0.0001$), indicating that > 20% of the ELIP were involved in complex formation.

The echogenicity of Ab-bELIP (anti-fibrinogen) was fully retained after complexation with NO-bELIP (Fig. 6). Addition of streptavidin to Ab-bELIP alone, which would be expected to form monotypic complexes, appeared to diminish the echogenicity somewhat. Data demonstrating that the biotin/avidin-mediated modular complex strategy succeeded in preserving targeted ELIP immunoreactivity are shown in Fig. 7. While there was no significant difference between the antigen reactivity of the control preparation and the NO-/Ab-bELIP complexes ($p > 0.05$), with a minimum average 70% retention, monotypic complexes exhibited significantly decreased immunoreactivity ($p = 0.01$).

Transwell passage of CD34+ human peripheral mononuclear cells through TNFα-stimulated human coronary artery endothelial cell monolayers (Fig. 8) was more than doubled (relative to IgG-bELIP controls; $p < 0.02$) by inclusion of BF-bELIP targeted to both CD34 and ICAM-1 prior to introduction of stem cells, followed by washes after each incubation step. Complexation of NO-bELIP to the BF-bELIP caused a more than twofold additional increase in transwell passage ($p < 0.002$). Such incremental stimulation of stem cell penetration after successive washing steps indicates that the enhanced endothelial permeability was caused by NO encapsulated in biotinylated liposomes bound to BF-bELIP through a streptavidin bridge.

4. Discussion

It is well known that proteins forced into close proximity with gases tend to denature, because the apolar environment provided by the juxtaposed gas does not favor the thermodynamically most stable configuration of the folded protein [25]. Consequently, gas entrapping microbubbles have proven difficult to target with protein ligands, because of denaturation during the microbubble preparation procedure [26]. This difficulty has been largely obviated by coupling the targeting ligands to preformed microbubbles using biotin/avidin linkage technology [27–29]. There is a similar propensity to denaturation of antibodies conjugated to liposomes, when subjected to pressurization and freeze-thawing procedures required to encapsulate bioactive gases (Fig. 1). Recently, Kheirolomoom *et al.* produced microbubble-liposome complexes, using biotin/avidin linkage technology, in order to improve the drug-delivery capacity of microbubbles [30,31], but the ability to enhance microbubble targeting capabilities by the same approach was also implied. Intrinsically echogenic liposomes (ELIP) compare favorably to microbubbles in terms of *in vivo* stability and targeting capabilities, as well as drug and gene delivery capacities [10,12,14,30]. Thus, utilization of the biotin/avidin linkage strategy to form multi-liposomal complexes may not only surmount the barrier to site-specific delivery of bioactive gases encapsulated in ELIP, but also may enhance the utility and versatility of the ELIP technology's therapeutic potential.

A 4:1 ratio of available biotin between gas-loaded and targeted ELIP, respectively, with an equal proportion, by weight, of both types of liposomes was chosen to favor formation of complexes likely to feature targeted ELIP modules at the surface, where they would be available for binding to their molecular targets. Fluorescence deconvolution microscopy confirmed that, while targeted modules were not preferentially situated on the complex periphery, some were available for binding at the surface in most aggregates. Although some large aggregates of up to 500 liposomes were observed, most were ≤ 3 μm in diameter. Beckman Coulter Multisizer 3 analysis indicated that more than 20% of liposomes were aggregated, but that complexes ≥ 2 μm in size comprised 2.4% of the particle population, suggesting that the average aggregate consisted of approximately 8 liposomes, which is consistent with the observed size of the complexes. Dual-labeled particles enumerated by flow cytometry comprised 1.2% of the total, further suggesting that half of the complexes were monotypic. As expected for biotin-avidin interactions, which are characterized by very high affinity associations, the complexation process was essentially complete within one minute.

This study demonstrates that the primary aim of the modular complex strategy was achieved, namely, bioactive gas delivery with essentially full retention of echogenicity and targeting capabilities. Both characteristics were somewhat decreased in monotypic targeted ELIP complexes, produced by addition of streptavidin to Ab-bELIP, without NO-loaded bELIP modules, probably because of steric factors. Interestingly, no such impairment was seen with the mixed aggregates, confirming that a sufficient proportion of targeting modules was maintained on the periphery of complexes to preserve their targeting capacity and that the NO-loaded bELIP were highly echogenic. More important, a 225% enhancement of bifunctional ELIP-potentiated stem cell passage through endothelial cell monolayers *in vitro* demonstrated the functional utility of the modular complex strategy, while simultaneously supporting several hypotheses. First, modular ELIP complexes can deliver liposome-encapsulated bioactive gases to specific cellular sites. Second, nitric oxide delivered in this manner increased the permeability of endothelial cell monolayers to stem cells, establishing a mode of enhanced perivascular and intravascular delivery of a range of therapeutic agents, including entire cells.

We had developed bifunctionally targeted liposomes, conjugated to antibodies specific for both a stem cell marker and an adhesion molecule expressed by inflammatory endothelium (in this case, CD34 and ICAM-1, respectively), as a means of bridging stem cells and atheroma, thus directing the former to sites where they could ameliorate pathological processes [32,33]. Besides testing the first hypothesis (BF-ELIP bridging function) mentioned above, the transwell experimental system employed in this study offered an effective means for testing the ability of the targeted ELIP modular complex strategy to increase endothelial permeability at the extreme of its therapeutic potential. In these experiments, the number of HMNC migrating through endothelial cell monolayers under conditions of NO-enhanced permeability was relatively consistent (CV = 21% for 3 experiments), while variability was higher (CV > 35%) without site-specific NO enhancement, suggesting a contribution of inter-experimentally variable endothelial and stem cell factors.

Now that *in vitro* methods for evaluation of ELIP modular complexes have been developed, optimal biotinylation ratios and module proportions can be determined. Further enhancement of stem cell delivery, as well as that of other agents, using ultrasound protocols will also be studied. In addition, the ELIP modular complex strategy has great potential for facilitating targeted delivery of therapeutic agents that may otherwise interfere with targeting strategies, not only for liposomes, but also for particulate formulations in general.

Supplementary Material

Refer to Web version on PubMed Central for supplementary material.

Acknowledgments

This work was supported, in part, by grants from the National Institutes of Health, R01 HL074002, HL059586 and NS047603. Fluorescence deconvolution microscopy was performed by Brian Poindexter of the Image Core Laboratory, UTHSC-H; flow cytometry procedures were performed by Dr. Luis Vence of the Immune Monitoring Core Laboratory, MD Anderson Cancer Center. Both facilities are components of the Center for Clinical and Translational Science, which is supported by NIH CTSA 5KL2RR024149-02.

References

1. Fischer JW, Hawkins S, Clowes AW. Pharmacologic inhibition of nitric oxide synthases and cyclooxygenases enhances intimal hyperplasia in balloon-injured rat carotid arteries. J Vasc Surg 2004;40(1):115–122. [PubMed: 15218471]
2. Rudic RD, Shesely EG, Maeda N, Smithies O, Segal SS, Sessa WC. Direct evidence for the importance of endothelium-derived nitric oxide in vascular remodeling. J Clin Invest 1998;101(4):731–736. [PubMed: 9466966]
3. Miller MR, Megson IL. Recent developments in nitric oxide donor drugs. British journal of pharmacology 2007;151(3):305–321. [PubMed: 17401442]
4. Radomski MW, Palmer RM, Moncada S. Endogenous nitric oxide inhibits human platelet adhesion to vascular endothelium. Lancet 1987;2(8567):1057–1058. [PubMed: 2889967]
5. Tsao PS, McEvoy LM, Drexler H, Butcher EC, Cooke JP. Enhanced endothelial adhesiveness in hypercholesterolemia is attenuated by L-arginine. Circulation 1994;89(5):2176–2182. [PubMed: 8181143]
6. Griffiths MJ, Evans TW. Inhaled nitric oxide therapy in adults. The New England journal of medicine 2005;353(25):2683–2695. [PubMed: 16371634]
7. Alkan-Onyuksel H, Demos SM, Lanza GM, Vonesh MJ, Klegerman ME, Kane BJ, Kuszak J, McPherson DD. Development of inherently echogenic liposomes as an ultrasonic contrast agent. Journal of pharmaceutical sciences 1996;85(5):486–490. [PubMed: 8742939]
8. Buchanan KD, Huang S, Kim H, Macdonald RC, McPherson DD. Echogenic liposome compositions for increased retention of ultrasound reflectivity at physiologic temperature. J Pharm Sci 2008;97(6): 2242–2249. [PubMed: 17894368]
9. Hamilton A, Rabbat M, Jain P, Belkind N, Huang SL, Nagaraj A, Klegerman M, Macdonald R, McPherson DD. A physiologic flow chamber model to define intravascular ultrasound enhancement of fibrin using echogenic liposomes. Investigative radiology 2002;37(4):215–221. [PubMed: 11923644]
10. Huang SL, Hamilton AJ, Pozharski E, Nagaraj A, Klegerman ME, McPherson DD, MacDonald RC. Physical correlates of the ultrasonic reflectivity of lipid dispersions suitable as diagnostic contrast agents. Ultrasound Med Biol 2002;28(3):339–348. [PubMed: 11978414]
11. Hamilton AJ, Huang SL, Warnick D, Rabbat M, Kane B, Nagaraj A, Klegerman M, McPherson DD. Intravascular ultrasound molecular imaging of atheroma components in vivo. J Am Coll Cardiol 2004;43(3):453–460. [PubMed: 15013130]
12. Huang S, Hamilton AJ, Tiukinhoy SD, Nagaraj A, Kane BJ, Klegerman M, McPherson DD, MacDonald RC. Liposomes as ultrasound imaging contrast agents and as ultrasound-sensitive drug delivery agents. Cell Mol Biol Lett 2002;7(2):233–235. [PubMed: 12097929]
13. Huang SL, Kee P, Kim H, Moody MR, Chrzanowski SM, MacDonald RC, McPherson DD. Nitric oxide loaded echogenic liposomes for nitric oxide delivery and inhibition of intimal hyperplasia. J Am Coll Cardiol 2009;54(7):652–659. [PubMed: 19660697]
14. Demos SM, Alkan-Onyuksel H, Kane BJ, Ramani K, Nagaraj A, Greene R, Klegerman M, McPherson DD. In vivo targeting of acoustically reflective liposomes for intravascular and transvascular ultrasonic enhancement. J Am Coll Cardiol 1999;33(3):867–875. [PubMed: 10080492]
15. Demos SM, Onyuksel H, Gilbert J, Roth SI, Kane B, Jungblut P, Pinto JV, McPherson DD, Klegerman ME. In vitro targeting of antibody-conjugated echogenic liposomes for site-specific ultrasonic image enhancement. J Pharm Sci 1997;86(2):167–171. [PubMed: 9040090]
16. Hamilton A, Huang SL, Warnick D, Stein A, Rabbat M, Madhav T, Kane B, Nagaraj A, Klegerman M, MacDonald R, McPherson D. Left ventricular thrombus enhancement after intravenous injection

of echogenic immunoliposomes: studies in a new experimental model. Circulation 2002;105(23): 2772–2778. [PubMed: 12057993]

17. Klegerman ME, Huang S, Parikh D, Martinez J, Demos SM, Onyuksel HA, McPherson DD. Lipid contribution to the affinity of antigen association with specific antibodies conjugated to liposomes. Biochim Biophys Acta 2007;1768(7):1703–1716. [PubMed: 17509522]
18. Lasche, J.; Weissig, V.; Brandl, M. Torchilin VP, WV., editor. New York, NY: Liposomes, Oxford University Press; 2003.
19. Klegerman ME, Hamilton AJ, Huang SL, Tiukinhoy SD, Khan AA, MacDonald RC, McPherson DD. Quantitative immunoblot assay for assessment of liposomal antibody conjugation efficiency. Anal Biochem 2002;300(1):46–52. [PubMed: 11743691]
20. Underwood PA. Problems and pitfalls with measurement of antibody affinity using solid phase binding in the ELISA. J Immunol Methods 1993;164(1):119–130. [PubMed: 8360501]
21. Bick RJ, Poindexter BJ, Schiess MC. Localization of calcitonin gene-related peptide in cardiomyocytes: comparison of neonatal and dedifferentiating cells to adult myocytes. Peptides 2005;26(2):331–336. [PubMed: 15629546]
22. Bick RJ, Poindexter BJ, Kott MM, Liang YA, Dinh K, Kaur B, Bick DL, Doursout MF, Schiess MC. Cytokines disrupt intracellular patterns of Parkinson's disease-associated proteins alpha-synuclein, tau and ubiquitin in cultured glial cells. Brain Res 2008;1217:203–212. [PubMed: 18501880]
23. Poindexter BJ. Immunofluorescence deconvolution microscopy and image reconstruction of human defensins in normal and burned skin. J Burns Wounds 2005;4:e7. [PubMed: 16921412]
24. Klegerman ME, Zou Y, McPherson DD. Sterilization of targeted echogenic liposomes with full retention of clinically relevant characteristics. AAPS J 2009;11(S1) Abstr 270.
25. Clarkson JR, Cui ZF, Darton RC. Protein Denaturation in Foam. J Colloid Interface Sci 1999;215(2): 323–332. [PubMed: 10419667]
26. Klibanov AL. Ligand-carrying gas-filled microbubbles: ultrasound contrast agents for targeted molecular imaging. Bioconjug Chem 2005;16(1):9–17. [PubMed: 15656569]
27. Lanza GM, Wickline SA. Targeted ultrasonic contrast agents for molecular imaging and therapy. Prog Cardiovasc Dis 2001;44(1):13–31. [PubMed: 11533924]
28. Lindner JR, Song J, Christiansen J, Klibanov AL, Xu F, Ley K. Ultrasound assessment of inflammation and renal tissue injury with microbubbles targeted to P-selectin. Circulation 2001;104 (17):2107–2112. [PubMed: 11673354]
29. Rychak JJ, Klibanov AL, Ley KF, Hossack JA. Enhanced targeting of ultrasound contrast agents using acoustic radiation force. Ultrasound Med Biol 2007;33(7):1132–1139. [PubMed: 17445966]
30. Huang SL. Liposomes in ultrasonic drug and gene delivery. Adv Drug Deliv Rev 2008;60(10):1167–1176. [PubMed: 18479776]
31. Kheirolomoom A, Dayton PA, Lum AF, Little E, Paoli EE, Zheng H, Ferrara KW. Acoustically-active microbubbles conjugated to liposomes: characterization of a proposed drug delivery vehicle. J Control Release 2007;118(3):275–284. [PubMed: 17300849]
32. Klegerman ME, Zou Y, Huang S, Shelat HS, Geng YJ, McPherson DD. Bifunctional targeting of echogenic immunoliposomes for directed stem cell delivery. J Am Coll Cardiol 2008;51:A288–A289.
33. Herbst SM, Klegerman ME, Kim H, Qi J, Shelat HS, Wassler M, Moody MR, Yang CM, Ge X, Zou Y, Kopechek JA, Clubb FJ, Kraemer DC, Huang S, Holland CK, McPherson DD, Geng YJ. Delivery of stem cells to porcine arterial wall with echogenic liposomes conjugated to antibodies against CD34 and intercellular adhesion molecule-1. Mol Pharm. In Press; doi:10.1021/mp900116r.

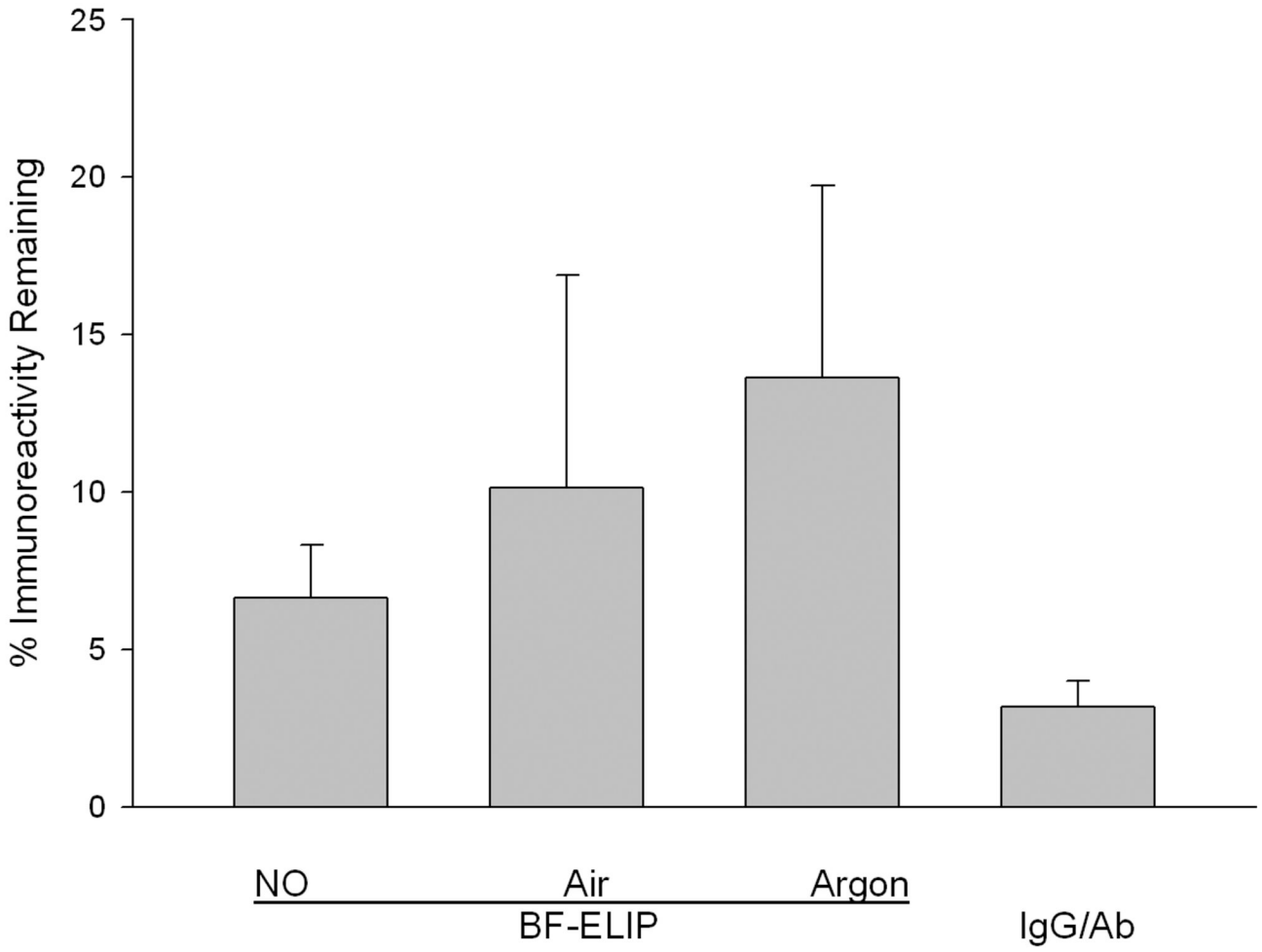

Figure 1.
Effect of gas treatment on antiICAM-1 immunoreactivity. The reactivity of antiICAM1-conjugated ELIP, pressurized with various gases as described in Methods, was compared with untreated Ab-ELIP. IgG/Ab refers to a mixture of unconjugated antiICAM-1 and mouse IgG in the same proportions as were conjugated, subjected to the same NO pressurization procedure as the Ab-ELIP. Values are the mean of 6–9 determinations; bars = SD.

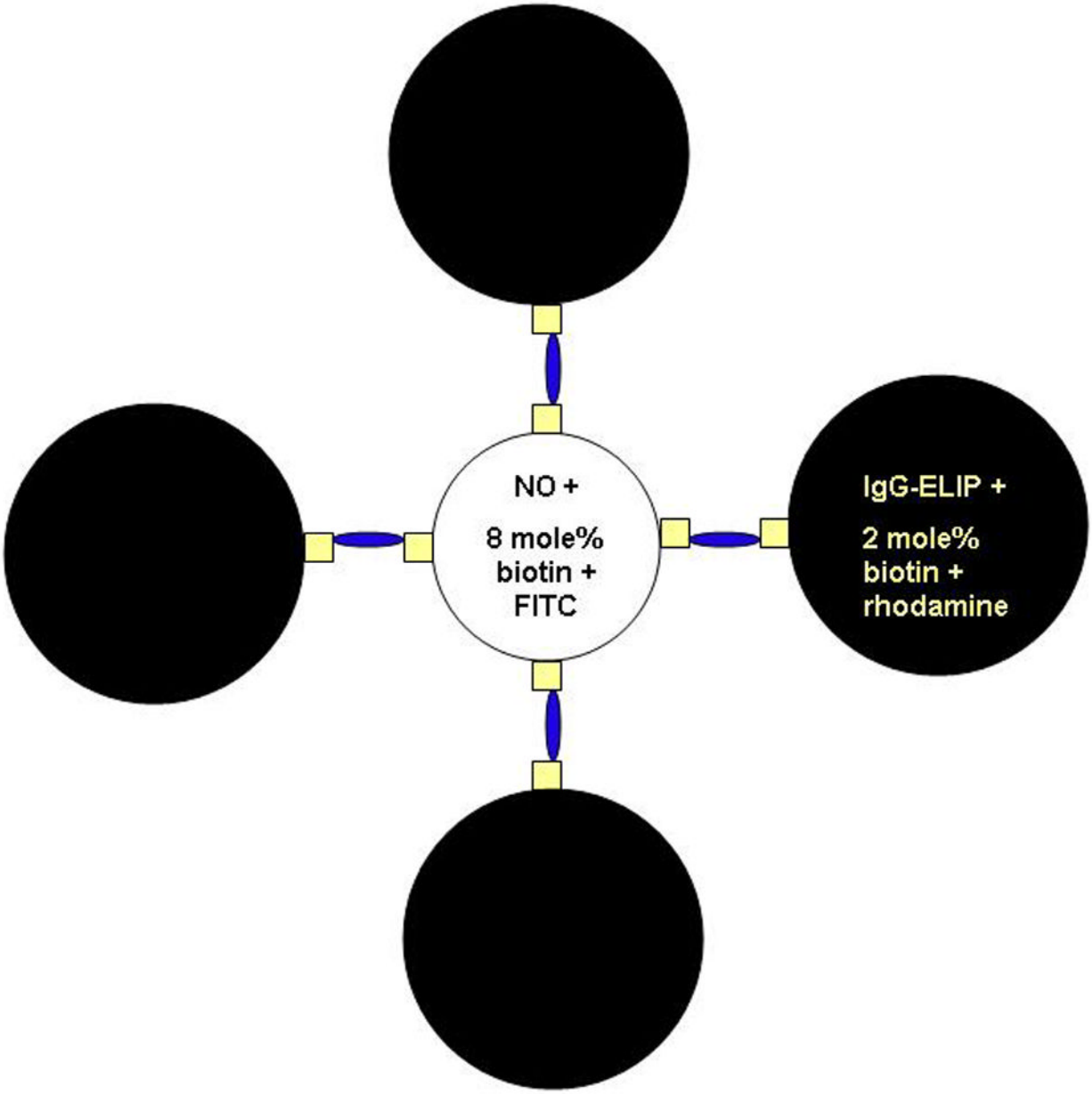

Figure 2.
Schematic representation of IgG-/NO-bELIP (biotinylated ELIP) modular complexes. Small squares represent biotin molecules; narrow ovals represent streptavidin bridges.

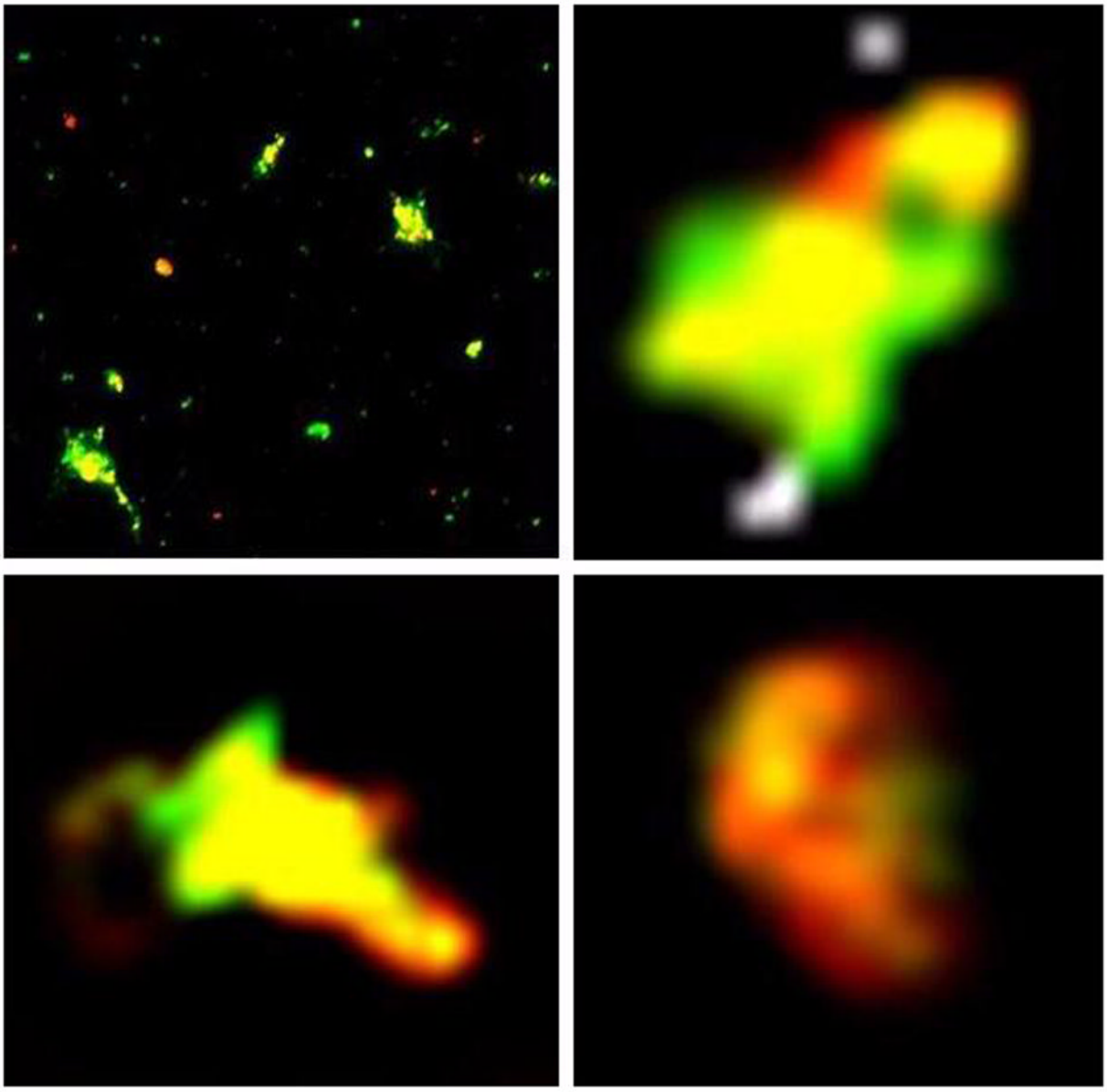

Figure 3.
Fluorescent microscopy of ELIP modular complexes formed from rhodamine B-labeled IgG-bELIP and fluoresceinated NO-loaded bELIP. Upper left panel: entire field of suspension 30 minutes after complex initiation; oil immersion with 100X objective. Scale: 1mm = 2μm. Remaining panels: deconvoluted images of individual complexes in the field. Scale: 1cm = 1μm.

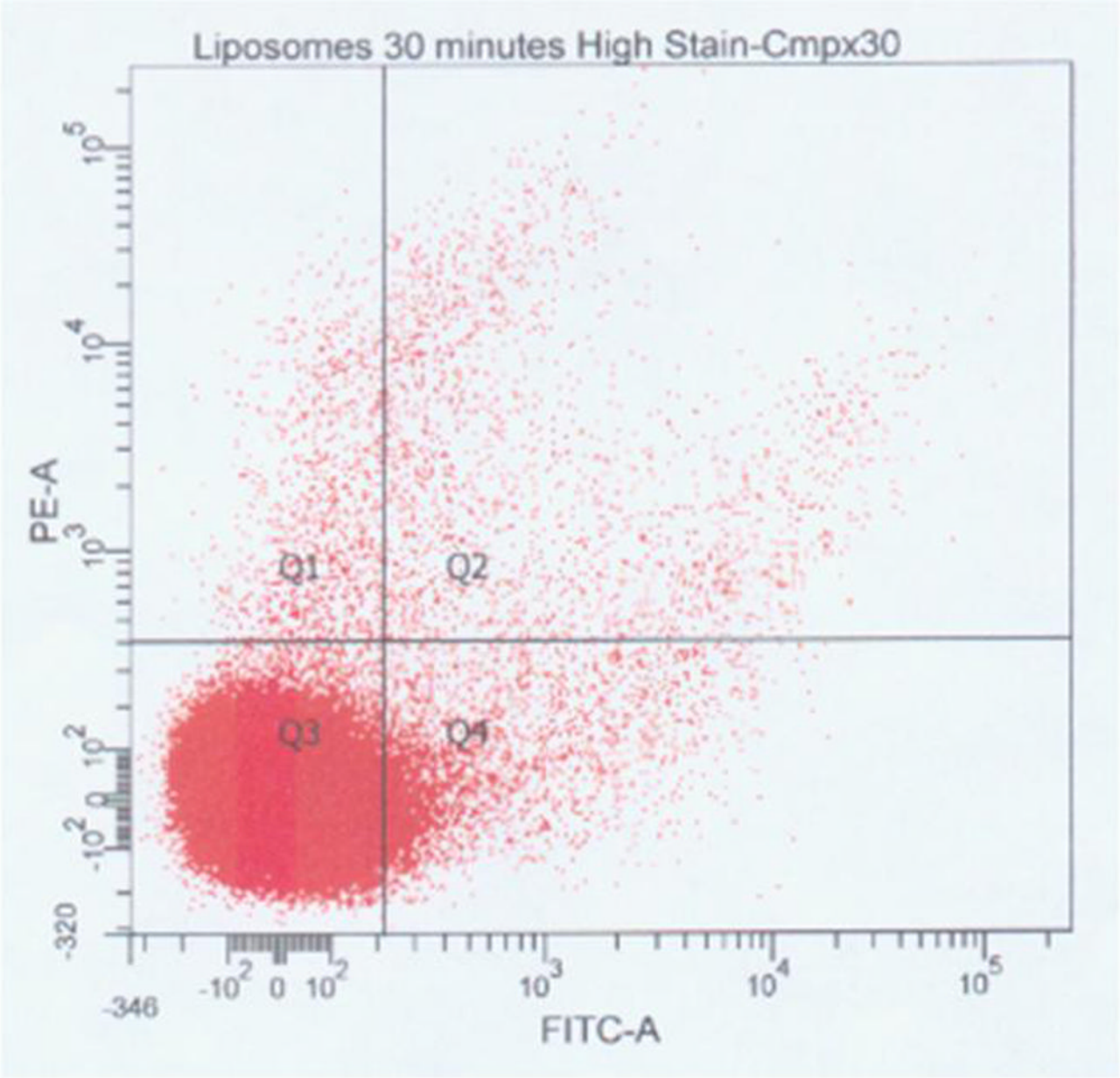

Figure 4.
Flow cytometry of ELIP modular complexes 30 minutes after initiation. Unlabeled IgG-bELIP was mixed with fluoresceinated NO-bELIP, complexed with streptavidin, and subsequently stained with anti-mouse IgG-phycoerythrin. Points in Quadrant 2 (Q2) represent mixed complexes.

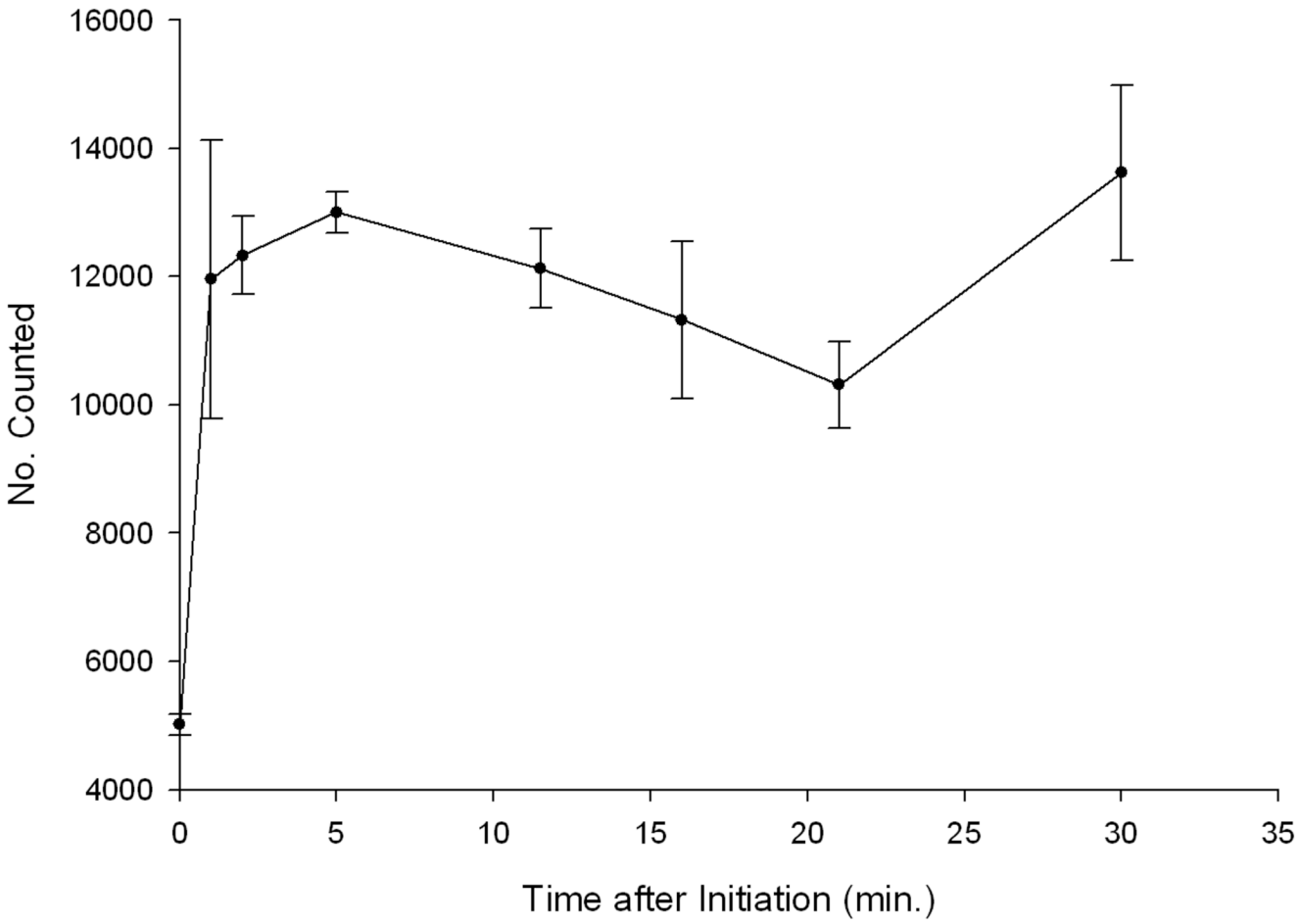

Figure 5.

Kinetic analysis of ELIP modular complex formation using the Beckman Coulter Multisizer 3. The number of particles of equivalent spherical diameter = 2–4 μm was measured at various time points after complex initiation. Each point represents the mean of 3 determinations (bars = SE). Particle number at 2 min. is significantly greater than at 0 min. ($p < 0.01$) and is significantly greater than that of a control consisting of mixed IgG-/NO-bELIP without added streptavidin ($p < 0.02$).

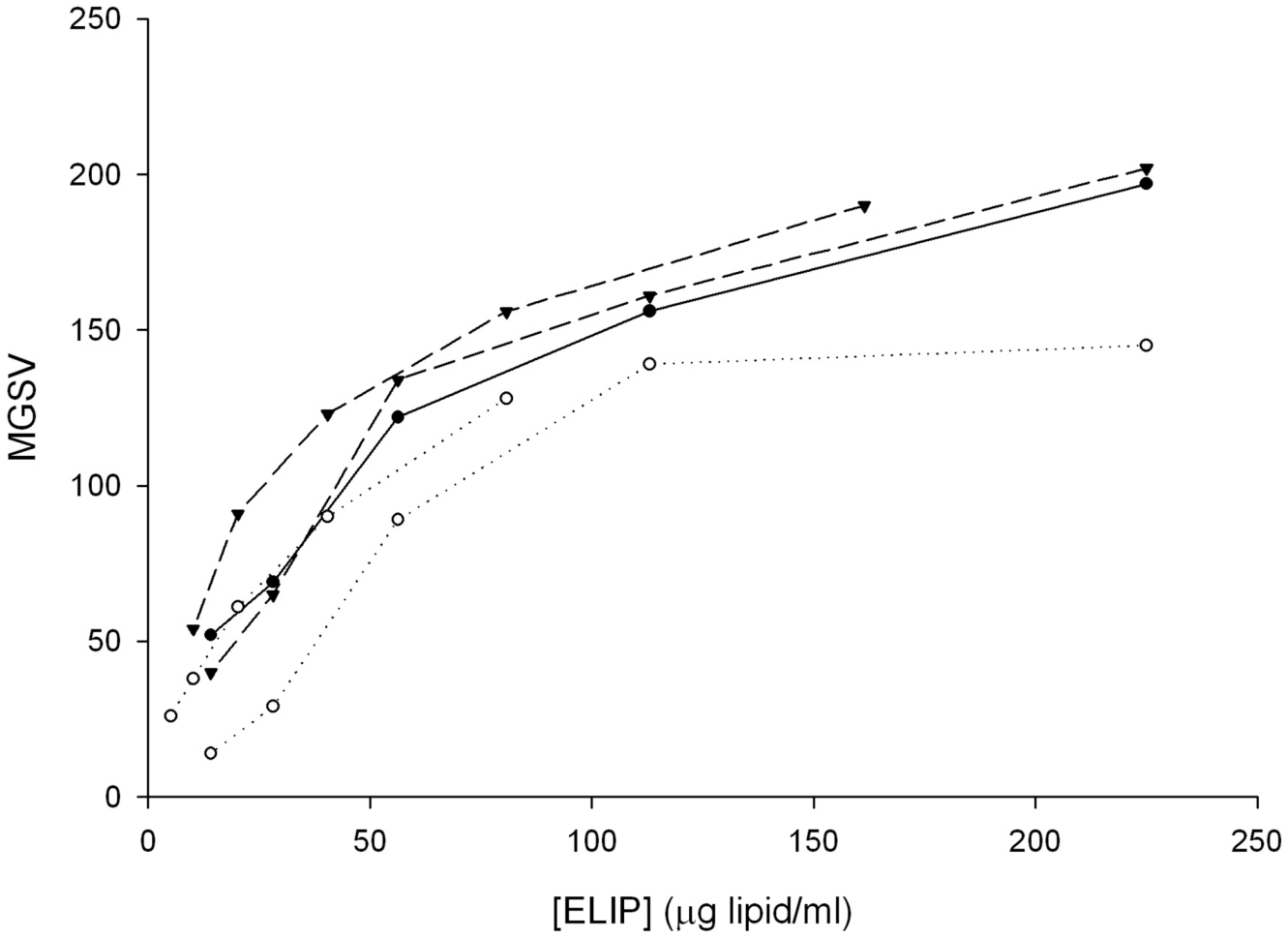

Figure 6.

Echogenicity of modular ELIP complexes. Densitometric representation of IVUS sonographic brightness, expressed as mean gray scale value (MGSV; 256-value scale), of anti-fibrinogen Abs conjugated to bELIP without NO-bELIP or streptavidin (closed circles, solid line; individual points from one experiment shown), Ab-bELIP with streptavidin only (open circles, dotted line; individual points from two experiments shown), and Ab-/NO-bELIP complexes (inverted triangles, dashed line; individual points from two experiments shown).

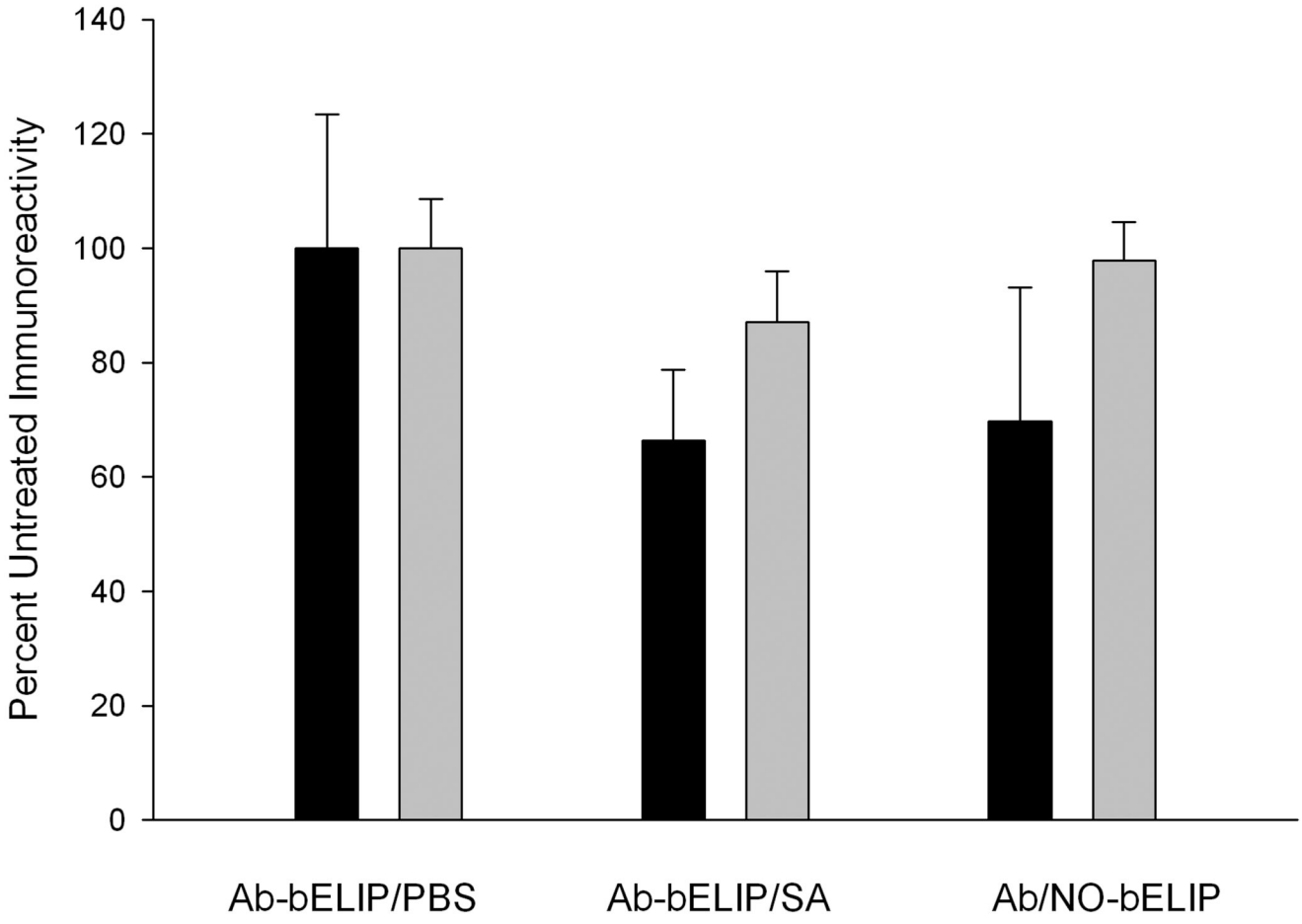

Figure 7.
Effect of nitric oxide-loaded biotinylated ELIP module coupling on antibody-conjugated ELIP immunoreactivity. Conjugated Ab: black = anti-fibrinogen; gray =antiICAM-1. Values are the means of 6–8 determinations ± SD.

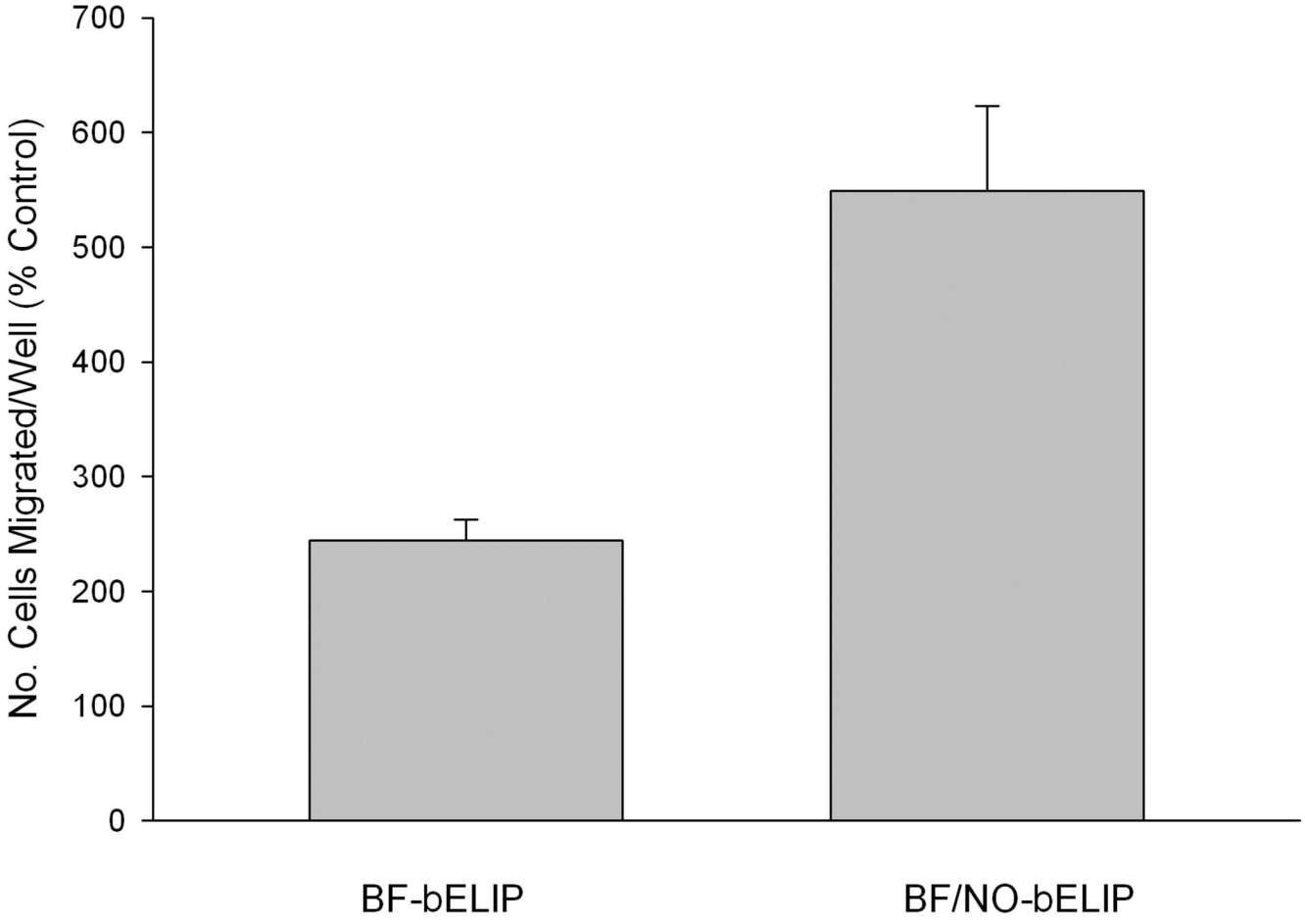

Figure 8.
Enhancement of BF-bELIP promotion of stem cell passage through endothelial cell monolayers by complexation of NO-loaded biotinylated ELIP. Data are normalized relative to the corresponding control (IgG-bELIP or IgG-/NO-bELIP). Values are the means of 9 determinations (in 3 experiments) ± SE.